

# Kinetic box models for the uptake of radionuclides and heavy metals by suspended particulate matter: equivalence between models and its implications

H. Barros <sup>a,\*</sup>, J.M. Abril <sup>b</sup>

<sup>a</sup> Nuclear Physics Laboratory, Universidad Simon Bolivar, P.O. 89000, Caracas 1080-A, Venezuela

<sup>b</sup> Dpto. Física Aplicada I, Universidad de Sevilla, EUITA, Carretera de Utrera km 1, C.P. 41013, Sevilla, Spain

## Abstract

In recent years an increasing experimental effort has been paid to the study of the sorption process of radionuclides and heavy metals by particulate matter in aquatic environments. This has led to the development of different kinetic box models. Most of them are variations of two basic approaches: one containing several (up to three) parallel reactions while the other involves consecutive reactions. All the reactions are reversible (irreversibility is contained as a particular case) with concentration independent coefficients. The present work provides analytical solutions and demonstrates that both approaches are mathematically equivalent. That is, both models produce the same analytical solution for the uptake curve (time course of the concentrations in the dissolved phase), which is illustrated using literature data. This result unifies the description of the observed behaviour, but it brings up the question of the physical meaning of the involved coefficients. Finally, the mathematical relationship developed here serves to discuss some limitations found in recent attempts in literature devoted to distinguish the actual uptake mechanism.

*Keywords:* Uptake kinetics; Box model; Radionuclides; Heavy metals; Aquatic environments

---

## 1. Introduction

Studies on the uptake kinetics of radionuclides and heavy metals by Suspended Particulate Matter (SPM) in aquatic environment are of increasing interest. They are essential to better understand the environmental behaviour of such inorganic pollutants in aquatic systems and to develop suitable predictive models. An accurate description of the uptake kinetics is particularly important in the following situations: Dispersion of radionuclides and heavy metals in aquatic systems with high SPM concentrations, during episodic enhancement of SPM concentrations (e.g., storms, heavy rain, or in some remedial actions), when the input of pollutants affects large areas (e.g., atmospheric deposition), or when the contaminated particles (SPM or sediments) becomes a delayed source of pollutants (desorption scenarios). These studies are also of great relevance in performance assessments for radioactive waste repositories.

---

\* Corresponding author. Tel./fax: +58 212 9063590.

E-mail address: hbarros@usb.ve (H. Barros).

The box model approach has been widely used to successfully describe the uptake kinetics. One can distinguish between parallel and consecutive reactions models, as summarized in Fig. 1. In this figure, the models involve up to three reversible reactions (the quality of experimental data can rarely justify more complex models). Obviously, irreversibility is contained as a particular case. The same is true for models containing only one or two reactions. The experimental approach usually consists in the spiking of the studied suspension to record the time course of the tracer concentrations in the dissolved phase. In general, a fitting procedure to the uptake curve is used to determine both the type of model to be used and the numerical values of the kinetic coefficients. This method can also support interesting discussions on the effects of different parameters (salinity, pH, specific surface area, etc). As a result, scientific literature presents a sparse set of models describing a wide variety of behaviours, even for the same tracer element, as it is summarized in what follows.

Nyffler et al. (1984) described the uptake kinetics in marine waters in terms of a single reversible reaction model, with excellent results for a large set of elements. These authors also used a reversible reaction followed by a consecutive irreversible channel for another group of radioisotopes. Benes and Cernik (1992) described the behaviour of radionuclides sorption ( $^{58}\text{Co}$ ,  $^{85}\text{Sr}$  and  $^{137}\text{Cs}$ ) onto natural particles in rivers in terms of parallel and consecutive kinetic 3-box models (or two reactions' models).

Comans and Hockley (1992) studied caesium sorption on illite and discussed the effect of competitive ions. They pointed out that reversibility was affected by slow kinetic and they used models incorporating a Freundlich isotherm and other based on a 2-box model plus a consecutive irreversible process. These authors also used 3 and 4-box models to identify different pathways or channels for the sorption onto the particles.

Laissaoui et al. (1998) studied the effect of salinity and pH in the sorption process for  $^{133}\text{Ba}$  by estuarine SPM using a single reversible (2-box) model.

Ciffroy et al. (2001) applied a consecutive 3-box model to satisfactorily describe the kinetics of adsorption and desorption of a set of six metallic radioisotopes. Other examples are given in the multiple parallel reactions proposed by Konoplev et al. (1992) and in the study performed by Stephens et al. (1998) applied to sediments.

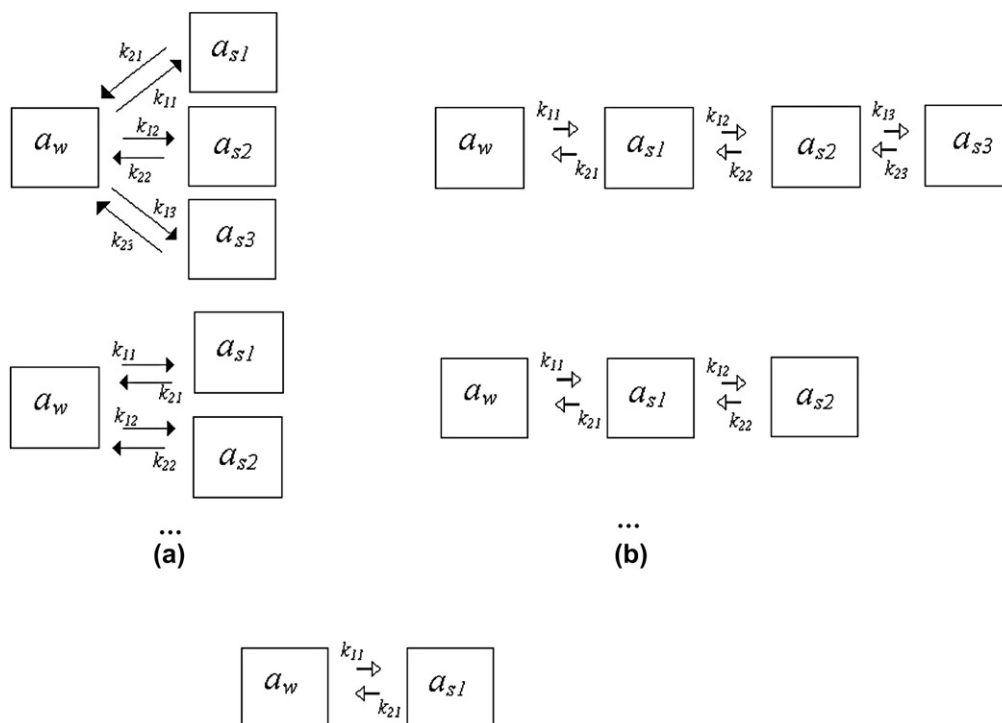


Fig. 1. Schematic (a) Parallel and (b) Consecutive Reversible Reaction Models.  $a_w$  represents the liquid phase concentration, while  $a_{si}$  are the concentrations in the different sites of the particle. The general case include four compartments which are needed to describe a 3-step uptake. Below it is shown a three compartment (2-step uptake) model as a particular case. Finally the simplest model (one reversible reaction) can be seen as a particular case for the two schemes.

In an interesting experimental work, Børretzen and Salbu (2000) estimated the apparent rate coefficients for 3-box parallel and consecutive models in terms of a post-sorption sequential extraction scheme. In a latter work Børretzen and Salbu (2002) studied the application of semi-Markov and Markov stochastic process coupled with 3-step parallel and consecutive box models in order to explain the residence times of Cs in a seawater–sediment system.

El Mrabet et al. (2001) presented a 4-box model to explain the uptake kinetics of Pu in natural aqueous suspensions. An extensive experimental work presented by Bunker et al. (2001) includes Co, Sr, Ru and Cs. In this study a linearization approach is compared with a consecutive 2, 3 or 4-box model, although in some cases the first reversible reaction is considered too fast and later substituted by a distribution coefficient.

Finally, numerous contributions apply these models to the transport of pollutants in waters and sediments: Benes et al. (1994), Smith and Comans (1996), Periañez and Martínez-Aguirre (1997), Periañez and Elliot (2002), Monte et al. (2006), Sasina et al. (2007), etc.

The present work provides analytical solutions for parallel and consecutive box models. Both models produce the same analytical solution for the uptake curve. The solutions for the solid-compartments are different but they show a similar behaviour, as it will be illustrated using literature data. This result unifies the description of the observed behaviour, but it brings up the question of the physical meaning of the involved coefficients. Finally, the present results serve to discuss some limitations found in recent attempts in literature devoted to distinguish the actual uptake mechanism.

## 2. Mathematical equivalence of parallel and consecutive kinetic box models

### 2.1. Basic assumptions for kinetic box models

Abril (1998) presented a microscopic theory for the uptake kinetics of radionuclides by SPM providing a basic understanding of these processes. Thus, adsorption of dissolved ions is considered as a statistical result due to collisions, which can be followed by physical or chemical adsorption with a certain probability. Typical kinetic box models assume that concentrations of pollutants are small enough to remain far from saturation and they consider only first order reactions. This implies that the concentration's change rate is proportional to the concentrations. Each box in the model represents different sites (by their chemical properties or different accessibility – e.g. inner surface of pores and free edges) where the studied ion can be bound. Different types of reactions can connect these sites. Different simultaneous reactions having similar time scales can be described through a single effective coefficient since the pollutant concentration can be extracted as a common factor in a first order equation. Finally, the concentrations of other species that takes place in the reaction can be considered constant, since the pollutant will interact mainly with natural elements that are present in large amounts.

The validity and applications for the involved kinetic coefficients is constrained to be local. Thus, they are dependent of the SPM concentration, the Specific Surface Area (SSA), mineralogical composition, geometry of pores and free edges, and on the chemical properties of water (pH, COC, anions, competitive cations, ...). Then, a full sample characterization can be very helpful to study those factors affecting the kinetic coefficients. This could serve to adapt their values within the range of variability of the environmental conditions. Furthermore, even restricted to their local significance, the so calibrated kinetic box models are very valuable tools in the strategies for the protection of natural aquatic ecosystems.

On the basis of the large list of experiments and observations already presented in literature, it can be considered as a general case that the adsorption of dissolved species by suspended particles is a process with up to three time scales, usually: minutes, hours and days. On the other hand, the experimental difficulties in measuring inside the different compartments that represent the particle limit the available experimental data. Thus, the discussion and analysis are generally presented on the basis of the water concentration records.

### 2.2. Parallel Reversible Reaction (PRR) model

To deal with an uptake process with three different characteristic times, it is necessary to use four compartments. The PRR model (Fig. 1a) assumes that all the reactions occur in parallel, being independent one from another. The only link between them is the available amount of dissolved ions. Let's say that there is a fast process, a moderate

one, and a slow one, being the corresponding particle compartments labelled by “1”, “2” and “3”, respectively. The governing equations for the tracer concentration in each compartment are:

$$\begin{aligned} \dot{a}_w &= -k_{11} \cdot a_w + k_{21} \cdot a_{s1} - k_{12} \cdot a_w + k_{22} \cdot a_{s2} - k_{13} \cdot a_w + k_{23} \cdot a_{s3} \\ \dot{a}_{s1} &= +k_{11} \cdot a_w - k_{21} \cdot a_{s1} \\ \dot{a}_{s2} &= +k_{12} \cdot a_w - k_{22} \cdot a_{s2} \\ \dot{a}_{s3} &= +k_{13} \cdot a_w - k_{23} \cdot a_{s3} \end{aligned} \quad (1)$$

$a_w$  represents the concentration in the liquid phase, while  $a_{s1}$ ,  $a_{s2}$  and  $a_{s3}$  are the concentrations in the different sites of the particle linked through to the faster, the moderate and the slow reactions, respectively. All the concentrations will be expressed in mol L<sup>-1</sup> or equivalent units. The constant rates or kinetic coefficients  $k_{ij}$ , with dimensions of T<sup>-1</sup>, are assumed to be constant since the physical–chemical conditions of the experiment are constant too.

The solution of Eq. (1) can be found by means of its Laplace Transformation (LT), denoted by  $\tilde{a}_w(s)$ . We note that  $\text{LT}\{\dot{a}_w(t)\} = s \cdot \tilde{a}_w(s) - a_w(0)$ , and similarly for the other concentrations. Taking into account typical initial conditions in tracing experiments ( $a_w(0) > 0$ ;  $a_{s_i}(t=0) = 0$  for  $i = 1,2,3$ ), the Eq. (1) can be rewritten in the Laplace space (Eq. (2)).

$$\begin{aligned} s \cdot \tilde{a}_w - a_w(0) &= -k_{11} \cdot \tilde{a}_w + k_{21} \cdot \tilde{a}_{s1} - k_{12} \cdot \tilde{a}_w + k_{22} \cdot \tilde{a}_{s2} - k_{13} \cdot \tilde{a}_w + k_{23} \cdot \tilde{a}_{s3} \\ s \cdot \tilde{a}_{s1} &= +k_{11} \cdot \tilde{a}_w - k_{21} \cdot \tilde{a}_{s1} \\ s \cdot \tilde{a}_{s2} &= +k_{12} \cdot \tilde{a}_w - k_{22} \cdot \tilde{a}_{s2} \\ s \cdot \tilde{a}_{s3} &= +k_{13} \cdot \tilde{a}_w - k_{23} \cdot \tilde{a}_{s3} \end{aligned} \quad (2)$$

then, operating in the resulting equations, one can solve  $\tilde{a}_w(s)$  as

$$\tilde{a}_w(s) = \frac{s^3 + s^2 a + s b + c}{s [s^3 + s^2 \sum k_{ij} + s k_{II} + k_{III}]} a_w(0) \quad (3)$$

where  $a$ ,  $b$ ,  $c$ ,  $k_{II}$  and  $k_{III}$  are functions of the coefficients  $k_{ij}$ . Afterward Eq. (3) can be regrouped, solving the cubic equation in the last denominator, as follows:

$$\frac{\tilde{a}_w(s)}{a_w(0)} = \frac{A_1}{s - s_1} + \frac{A_2}{s - s_2} + \frac{A_3}{s - s_3} + \frac{1 - A_1 + A_2 + A_3}{s} \quad (4)$$

In Eq. (4) the constants  $A_i$  and  $s_i$  are functions of  $k_{ij}$  (the explicit relationships will be considered some further). Taking the Inverse Laplace Transformation, the corresponding solution is:

$$a_w(t) = a_w(0) [A_1 (e^{s_1 t} - 1) + A_2 (e^{s_2 t} - 1) + A_3 (e^{s_3 t} - 1) + 1] \quad (5)$$

This solution is a multi-exponential decay (note that the values  $s_i$ 's are negative), reducing the water concentration in three different stages. The simplification introduced by the initial conditions is justified since we are focusing on releases of anthropogenic pollutants, but the result can be easily extended for a more general situation. Similarly, the analytical solutions for the particle-associated concentrations can be stated as a linear combination of the same exponential functions.

Given the experimental uptake curve, it is possible to find out the characteristic frequencies and amplitudes ( $s_1, s_2, s_3, A_1, A_2, A_3$ ) by a fitting procedure using Eq. (5); and then, to relate these parameters with the corresponding kinetic coefficients involved in the model ( $k_{11}, k_{21}, k_{12}, k_{22}, k_{13}, k_{23}$ ). Let us introduce some auxiliary variables (related with Eq. (3)) in order to avoid unnecessary complicated expressions:

$$\begin{aligned} a &= s_1(A_1 - 1) + s_2(A_2 - 1) + s_3(A_3 - 1) \\ b &= s_1 s_2 + s_2 s_3 + s_1 s_3 - A_1 s_1 (s_2 + s_3) - A_2 s_2 (s_1 + s_3) - A_3 s_3 (s_1 + s_2) \\ c &= s_1 s_2 s_3 (A_1 + A_2 + A_3 - 1) \end{aligned} \quad (6)$$

Then,  $k_{ij}$  coefficients can be obtained as the solutions of the following equations:

$$\sum_{ij} k_{ij} = - \sum_l s_l$$

$$\begin{aligned}
k_{21}k_{22} + k_{21}k_{23} + k_{22}k_{23} + k_{11}(k_{22} + k_{23}) + k_{12}(k_{21} + k_{23}) + k_{13}(k_{21} + k_{22}) &= s_1s_2 + s_1s_3 + s_2s_3 \\
k_{21}k_{22}k_{23} + k_{11}k_{22}k_{23} + k_{12}k_{21}k_{23} + k_{13}k_{21}k_{22} &= -s_1s_2s_3 \\
k_{21} + k_{22} + k_{23} &= a \\
k_{21}k_{22} + k_{21}k_{23} + k_{22}k_{23} &= b \\
k_{21}k_{22}k_{23} &= c
\end{aligned} \tag{7}$$

It should be noted that in many works, a numerical scheme (as finite differences) was applied instead of the fitting to the analytical solution. This is clearly equivalent but in any case we have to ensure that there are enough experimental points in each stage (minutes, hours and days) to obtain a good description of the curve in the whole temporal range.

### 2.3. Consecutive Reversible Reaction (CRR) model

Let's suppose that the reactions are consecutive (Fig. 1b). In such situations the available amount of ions in each step depends on the previous process. In this case, the differential equations are

$$\begin{aligned}
\dot{a}_w &= -k_{11} \cdot a_w + k_{21} \cdot a_{s1} \\
\dot{a}_{s1} &= +k_{11} \cdot a_w - k_{21} \cdot a_{s1} - k_{12} \cdot a_{s1} + k_{22} \cdot a_{s2} \\
\dot{a}_{s2} &= +k_{12} \cdot a_{s1} - k_{13} \cdot a_{s2} - k_{22} \cdot a_{s2} + k_{23} \cdot a_{s3} \\
\dot{a}_{s3} &= +k_{13} \cdot a_{s2} - k_{23} \cdot a_{s3}
\end{aligned} \tag{8}$$

Once again, Eq. (5) gives the analytical solution and Eqs. (3), (4) and (6) can be applied. Then, it is possible to obtain the kinetic coefficients in terms of the multi-exponential curve's coefficients (amplitudes and frequencies) solving the following equations:

$$\begin{aligned}
\sum_{ij} k_{ij} &= -\sum_l s_l \\
k_{11}(k_{12} + k_{13} + k_{22} + k_{23}) + k_{22}(k_{23} - k_{12}) + (k_{12} + k_{21})(k_{13} + k_{22} + k_{23}) &= s_1s_2 + s_1s_3 + s_2s_3 \\
k_{11}k_{22}k_{23} + k_{11}k_{12}(k_{13} + k_{23}) + k_{21}k_{22}k_{23} &= -s_1s_2s_3 \\
k_{12} + k_{13} + k_{21} + k_{22} + k_{23} &= a \\
k_{22}k_{23} - k_{12}k_{22} + (k_{12} + k_{21})(k_{13} + k_{22} + k_{23}) &= b \\
k_{21}k_{22}k_{23} &= c
\end{aligned} \tag{9}$$

### 2.4. Equivalence between models

In scientific literature the fitting parameters are usually obtained from the observed time course of tracer concentrations in the dissolved phase. Since Eq. (5) is the solution in both cases, it is possible to generate the same analytical function  $a_w(t)$  using two different sets of kinetics coefficients regarded to *PRR* and *CRR* models, respectively. Then, the two models are mathematically equivalent in that approach. In other words, once obtained an uptake curve for water concentration, it is not possible to determine which mechanism is the cause of the phenomenology. This generates an important question about the physical meaning of the kinetic coefficients. Moreover, and despite the experimental limitations in distinguishing different concentrations within the particles, the analytical solutions for these compartments are not exactly the same, but their behaviour is very similar, as it will be shown some further.

From the Eqs. (7) and (9) an explicit relationship can be obtained between both set of coefficients. Eq. (10) illustrates such a relationship for the simple case of only two characteristic times (two reactions involving three boxes), which will support a further discussion:

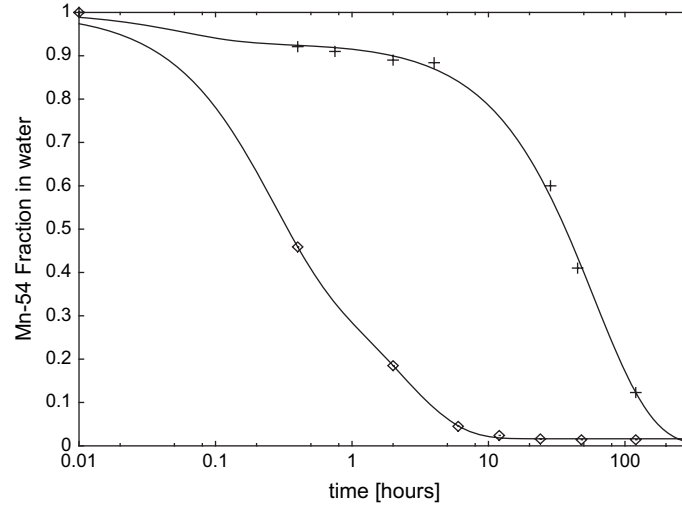


Fig. 2.  $^{54}\text{Mn}$  uptake in summer ( $\diamond$ ) and winter (+) seasons (data from Ciffroy et al., 2001). The higher particle concentration ( $2 \text{ g L}^{-1}$ ) corresponds to the stronger uptake ( $\diamond$ ), while the slower uptake (+) is due to a lower concentration ( $0.2 \text{ g L}^{-1}$ ). In both cases  $^{58}\text{Co}$  sorption by riverine SPM has been successfully fitted to a 2-step exponential decay (Eq. (2) restricted to 2-step), corresponding either to *CRR* or *PRR* models. The obtained coefficients are given in Table 1.

$$\begin{aligned}
 k_{11}^* &= k_{11} + k_{12} \\
 k_{21}^* &= \frac{k_{11}k_{21} + k_{12}k_{22}}{k_{11} + k_{12}} \\
 k_{22}^* &= k_{21}k_{22} \frac{k_{11} + k_{12}}{k_{11}k_{21} + k_{12}k_{22}} \\
 k_{12}^* &= k_{21} + k_{22} - \frac{k_{11}k_{21} + k_{12}k_{22}}{k_{11} + k_{12}} - k_{21}k_{22} \frac{k_{11} + k_{12}}{k_{11}k_{21} + k_{12}k_{22}}
 \end{aligned} \tag{10}$$

In Eq. (10)  $k_{ij}^*$  and  $k_{ij}$  correspond to the *CRR* and *PRR* models, respectively.

### 3. Applications of the *PRR* and *CRR* models

#### 3.1. Uptake with two characteristic times

Ciffroy et al. (2001) studied the effects in the  $^{54}\text{Mn}$  uptake due to seasonal changes in lacustrine SMP. Their experimental results (Fig. 2) will serve to illustrate the use of *CRR* and *PRR* models. For each experiment the  $^{54}\text{Mn}$

Table 1  
Characteristics times, amplitudes and their corresponding kinetic coefficients for two uptake experiments with  $^{54}\text{Mn}$ <sup>a</sup>

	Summer ( $R^2 = 0.99995$ ) <sup>d</sup>				Winter ( $R^2 = 0.998$ ) <sup>d</sup>				
Uptake curve <sup>b</sup>	$t_1$	$t_2$	$A_1$	$A_2$	$t_1$	$t_2$	$A_1$	$A_2$	
	0.234	2.309	0.583	0.401	0.0566	59.056	0.0695	0.929	
Box models <sup>c</sup>	$k_{11}$	$k_{21}$	$k_{12}$	$k_{22}$	$k_{11}$	$k_{21}$	$k_{12}$	$k_{22}$	
	<i>PRR</i>	1.776	2.024	0.885	0.0148	1.225	16.432	0.0182	0.000025
	<i>CRR</i>	2.661	1.356	0.661	0.0221	1.243	16.192	0.2402	0.000025

<sup>a</sup> Experiments from Ciffroy et al. (2001).

<sup>b</sup> Parameters given in Eq. (2). The  $A_i$ 's are dimensionless,  $t_i$  ( $t_i = -s_i^{-1}$ ) are given in hours (obtained by fitting).

<sup>c</sup> Models and coefficients defined in Fig. 1.  $k_{ij}$  values in  $\text{hour}^{-1}$ .

<sup>d</sup>  $R^2$  corresponds to the exponential fitting (Eq. (2)).

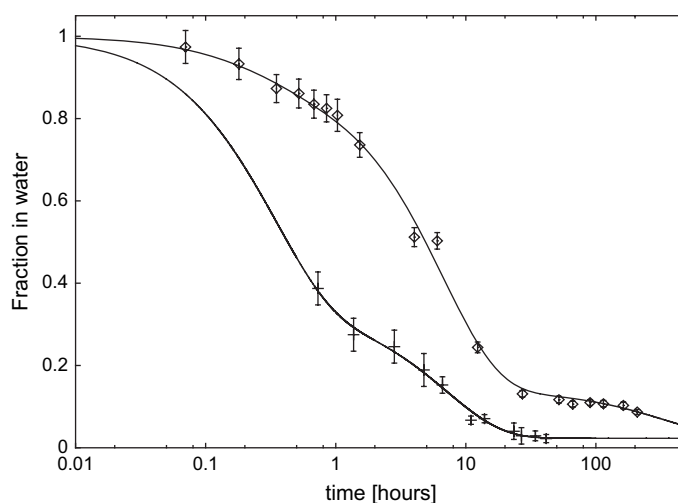


Fig. 3. Sorption of  $^{57}\text{Co}$  (+) by  $20 \text{ g L}^{-1}$  of lacustrine SPM (data from Bunker et al., 2001), and  $^{133}\text{Ba}$  ( $\diamond$ ) by  $10 \text{ g L}^{-1}$  of estuarine SPM (data from ENRESA, 2002). Lines correspond to the 3-step exponential fitting (Eq. (2)).

uptake curve has been successfully fitted to a second order exponential decay (shown in the same Fig. 2). Table 1 summarizes the curve parameters and the coefficients corresponding to the *CRR* and *PRR* models. Then, consecutive or parallel reactions can identically explain the data. In the referred work the authors performed desorption experiments and found some discrepancies between observations and the box model's predictions, although this could probably be related to some artefacts in the experimental method. In fact particles were filtered before the release or desorption experiment and it could cause agglomeration of the particles, leading to a reduction of both, the desorbed fraction and the exposed surface.

### 3.2. Uptake with three characteristic times

Bunker et al. (2001) reported uptake experiments with  $^{57}\text{Co}$  by suspended lacustrine sediments where it is possible to distinguish up to three different characteristic times. A similar behaviour has been found with  $^{133}\text{Ba}$  and estuarine sediments, as reported in the technical document by ENRESA (2002). The experimental data from these references appear in Fig. 3. They were fitted to a third order exponential decay (also in Fig. 3). Table 2 summarizes the corresponding *CRR* and *PRR* coefficients.

Bunker et al. (2001) used a distribution coefficient instead of a consecutive reversible reaction for the fast channel, perhaps because of their poor time resolution in the first hour interval (only one data point). This also limited the present modelling approach. Thus, only the ratio  $k_{d1} = k_{11}/k_{21}$  is well defined, and the numerical values for  $k_{11}$  and  $k_{21}$  shown in the table can be affected by a common multiplicative factor.

Table 2  
Characteristics times, amplitudes and kinetic coefficients for uptake experiments with  $^{133}\text{Ba}$  and  $^{57}\text{Co}$ <sup>a</sup>

	$^{133}\text{Ba}$ ( $R^2 = 0.997$ ) <sup>d</sup>						$^{57}\text{Co}$ ( $R^2 = 0.9994$ ) <sup>d</sup>					
Uptake curve <sup>b</sup>	$t_1$	$t_2$	$t_3$	$A_1$	$A_2$	$A_3$	$t_1$	$t_2$	$t_3$	$A_1$	$A_2$	$A_3$
	0.861	8.765	946.53	0.189	0.699	0.100	0.0796	0.346	7.056	0.0381	0.626	0.313
Box models <sup>c</sup>	$k_{11}$	$k_{21}$	$k_{12}$	$k_{22}$	$k_{13}$	$k_{23}$	$k_{11}$	$k_{21}$	$k_{12}$	$k_{22}$	$k_{13}$	$k_{23}$
<i>PRR</i>	0.365	3.388	0.124	0.019	0.0118	0.0007	0.331	12.169	1.636	1.091	0.365	0.009
<i>CRR</i>	0.501	2.472	0.909	0.025	0.0016	0.0007	2.332	2.492	6.269	4.171	0.325	0.011

<sup>a</sup> The experiment with  $^{133}\text{Ba}$  is from ENRESA (2002), while these with  $^{57}\text{Co}$  is from Bunker et al. (2001).

<sup>b</sup> Parameters given in Eq. (2). The  $A_i$ 's are dimensionless,  $t_i$  are given in hours (obtained by fitting).

<sup>c</sup> Models and coefficients defined in Fig. 1.  $k_{ij}$  values in  $\text{hour}^{-1}$ .

<sup>d</sup>  $R^2$  corresponds to the exponential fitting (Eq. (2)).

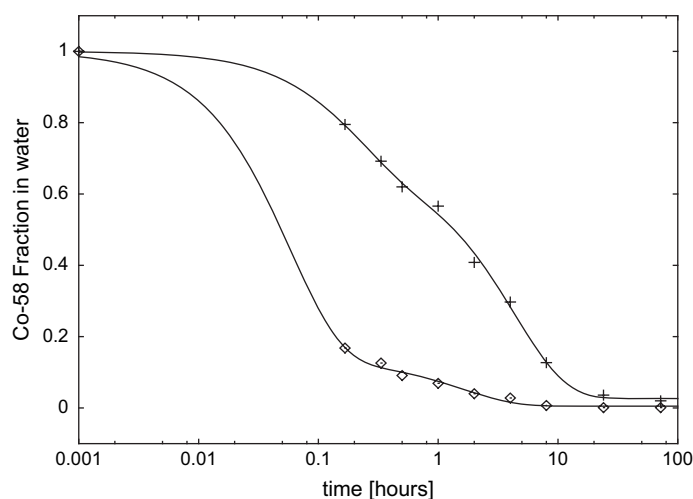


Fig. 4. Sorption of  $^{58}\text{Co}$  by riverine SPM (data from Benes and Cernik, 1992). SPM concentrations of  $0.2 \text{ g L}^{-1}$  (+) and  $2 \text{ g L}^{-1}$  ( $\diamond$ ). Lines correspond to a 2-step exponential fitting (Eq. (2) restricted to 2-step).

#### 4. Reviewing some attempts to distinguish between *PRR* and *CRR* models

##### 4.1. The effect of SPM concentration

Benes and Cernik (1992) carried out uptake experiments with  $^{58}\text{Co}$  varying concentrations of riverine SPM; they applied 2-steps *PRR* and *CRR* models. One could expect, as a first approach, that a change in the available surface for the uptake could serve to distinguish between both models.

The data from Benes and Cernik (1992) are shown in Fig. 4 along with the fits provided by Eq. (5) with two characteristic times, while the corresponding *PRR* and *CRR* coefficients appear in Table 3. We note that those authors found slight differences between *PRR* and *CRR* model fits, probably due to their numerical fitting algorithm, and they do not conclude their mathematical equivalence.

In the case of parallel reactions it is clear from the definition of the model, that the direct coefficients  $k_{11}$  and  $k_{12}$  should be proportional to the available particle's surface and consequently to the load concentration (when the particle size spectra is preserved). And a similar behaviour should be expected for the first direct coefficient  $k_{11}$  in the consecutive reaction model. Thus, Benes and Cernik (1992) conducted uptake experiments with different SPM concentrations and found linearity in the plots  $k_{1j}$  vs. SPM concentration. However, no conclusion was given about the

Table 3  
Exponential and model's coefficients for the experiments with  $^{58}\text{Co}$ <sup>a</sup>

	$2 \text{ g L}^{-1}, R^2 = 0.9994^{\text{d}}$				$0.2 \text{ g L}^{-1}, R^2 = 0.9984^{\text{d}}$			
Uptake curve <sup>b</sup>	$t_1$	$t_2$	$A_1$	$A_2$	$T_1$	$t_2$	$A_1$	$A_2$
	0.0575	1.614	0.866	0.129	0.202	4.323	0.326	0.648
Box models <sup>c</sup>	$k_{11}$	$k_{21}$	$k_{12}$	$k_{22}$	$k_{11}$	$k_{21}$	$k_{12}$	$k_{22}$
<i>PRR</i> -present work	11.449	2.856	3.677	0.0186	1.439	3.407	0.323	0.0089
<i>PRR</i> -Benes <sup>e</sup>	9.660	1.449	2.580	0.003	1.020	1.591	0.270	0.006
<i>CRR</i> -present work	15.126	2.166	0.684	0.0245	1.762	2.784	0.621	0.0108
<i>CRR</i> -Benes <sup>e</sup>	15.360	2.304	0.720	0.005	1.680	2.738	0.600	0.008

<sup>a</sup> Experiments from Benes and Cernik (1992).

<sup>b</sup> Parameters given in Eq. (2). The  $A_i$ 's are dimensionless,  $t_i$  are given in hours (obtained by fitting).

<sup>c</sup> Models and coefficients defined in Fig. 1.  $k_{ij}$  values in  $\text{hour}^{-1}$ .

<sup>d</sup>  $R^2$  corresponds to the exponential fitting (Eq. (2)).

<sup>e</sup> The coefficients obtained by the authors were originally presented in different units.



suitability of *PRR* or *CRR* models since once again both results were equally good. This apparent coincidence is easily explained by analyzing the mathematical relationship between the two sets of coefficients provided in Eq. (10). Then, it is clear that any increase of  $k_{11}$  and  $k_{12}$  by a given factor corresponds to the increasing of  $k_{11}^*$  by the same factor, preserving the last relationship and making impossible through that way the observation of any difference in the description of the concentrations in the dissolved phase.

#### 4.2. Distinguishing the particle-associated concentrations

As an approach to obtain information about the inner part of the particles, Børretzen and Salbu (2000) proposed a post-sorption sequential extraction scheme. In that paper, the amount of radionuclides extracted in several chemical steps is regrouped and operationally associated with the content of the compartments used in the model. Then, results for  $a_w$ ,  $a_{s1}$  and  $a_{s2}$  were overall fitted with *CRR* and *PRR* models (Figs. 5b and 6b). They used the first experimental measurement as initial conditions. This limits the predictive use of the model and will introduce an error source. Thus,

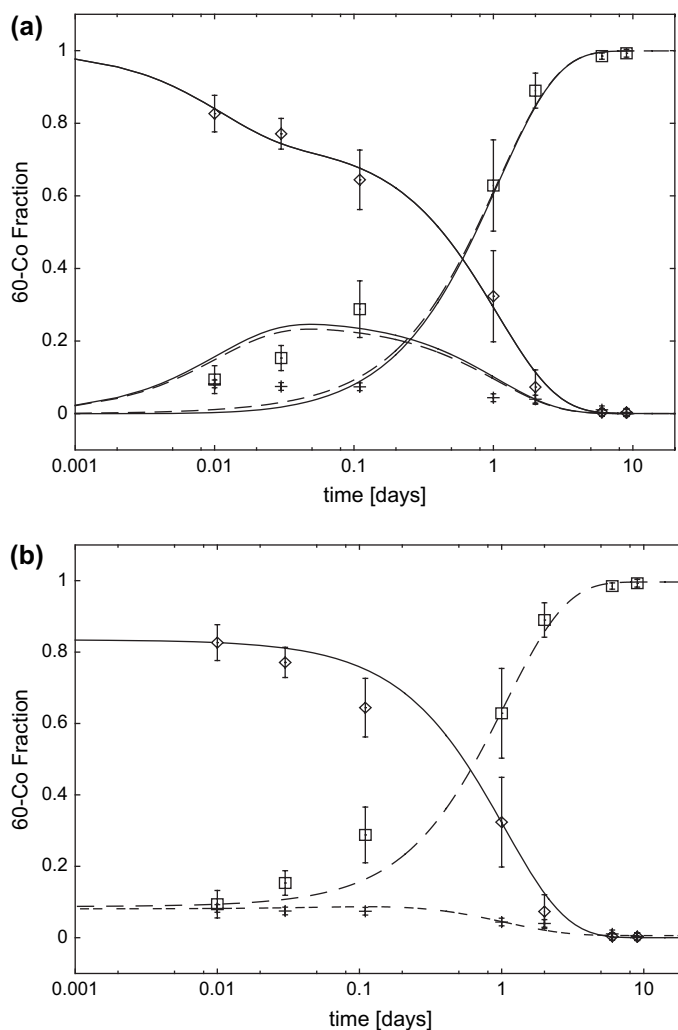


Fig. 5. Fractions of  $^{60}\text{Co}$  in the liquid phase  $a_w$  ( $\diamond$ ) and the two operationally defined compartments:  $a_{s1}$  is the reversible (+) and  $a_{s2}$  is the slowly reversible ( $\square$ ) bounded fraction. Experimental data from Børretzen and Salbu (2000). (a) Our fitting for  $a_w$  which includes the initial condition, here the  $a_{s1}$  and  $a_{s2}$  curves are predictions based on the coefficients extracted from the  $a_w$  curve. Note that *PRR* (dash lines) and *CRR* (solid lines) models give practically the same result (see text for details). Fig. 5b Børretzen and Salbu's fitting (only *CRR*), but in a semi-log scale and extrapolated to  $t=0$ .

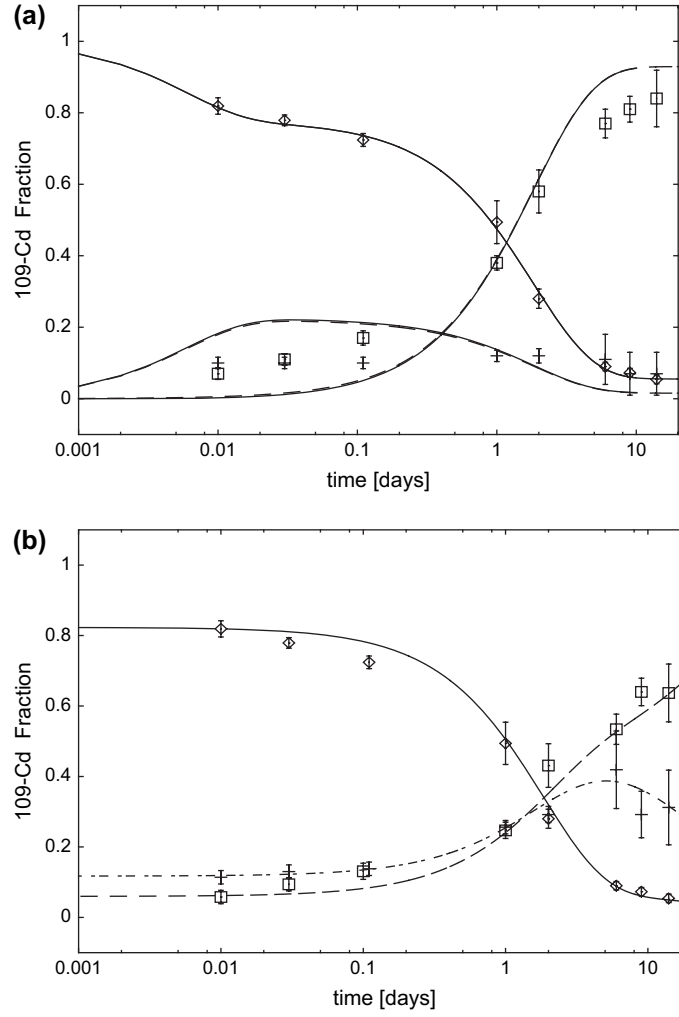


Fig. 6. Fractions of  $^{109}\text{Cd}$ :  $a_w$  ( $\diamond$ ),  $a_{s1}$  (+) and  $a_{s2}$  ( $\square$ ) (data from Børretzen and Salbu, 2000). (a) Our curves for the water fraction fitting and the prediction for the other compartments (dash PRR and CRR solid lines). Once again, the two models give a similar result. In this case it was changed the operational definition of those compartments, see text for details. (b) Børretzen and Salbu's fitting (only PRR) extrapolated to  $t=0$ .

although the curves presented in the original work were in agreement with the data, the known initial conditions ( $a_{s_i}(0) = 0$  and  $a_w/a_w(0) = 1$ ) cannot be reached when using the proposed models and coefficients.

On the other hand, it is possible to use only the liquid phase concentration ( $a_w$ ) curve, and then to obtain the behaviour of the particle-associated compartment as a model prediction. This is presented in Figs. 5a and 6a, where our

Table 4  
Exponential and model's coefficients for  $^{60}\text{Co}$ <sup>a</sup>

	Present work, $R^2 = 0.996^d$				Børretzen and Salbu			
Uptake curve <sup>b</sup>	$t_1$	$t_2$	$A_1$	$A_2$				
	0.011	1.062	0.250	0.750				
Box models <sup>c</sup>	$k_{11}$	$k_{21}$	$k_{12}$	$k_{22}$	$k_{11}$	$k_{21}$	$k_{12}$	$k_{22}$
PRR	21.985	67.878	1.249	0.0006				
CRR	23.234	64.228	3.650	0.0007	0.96	0	8.3	0.05

<sup>a</sup> Experiment from Børretzen and Salbu (2000).

<sup>b</sup> Parameters given in Eq. (2). The  $A_i$ 's are dimensionless,  $t_i$  are given in hours (obtained by fitting).

<sup>c</sup> Models and coefficients defined in Fig. 1.  $k_{ij}$  values in  $\text{days}^{-1}$ .

<sup>d</sup>  $R^2$  corresponds to the exponential fitting (Eq. (2)).

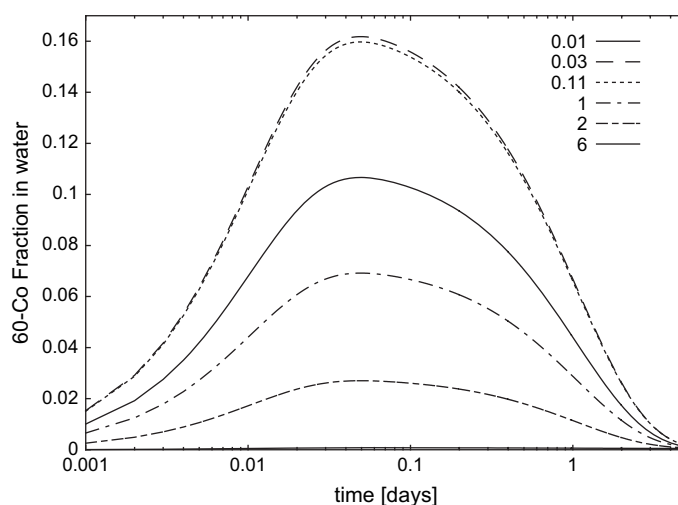


Fig. 7. Time course of the cobalt's desorbed fraction for different contact times (0.01 to 6 days). The prediction is based on the *PRR* and *CRR* models, obtaining the same mathematical description by using any one of them. The initial conditions for each curve correspond to a given contact time in the above mentioned experiment (Fig. 5) by Børretzen and Salbu (2000). Thus the obtained curves can be compared with the desorption data shown in Table 5.

*CRR* and *PRR* curves for  $a_w$  overlap, while for  $a_{s1}$  and  $a_{s2}$  both models provide a similar solution. We note that the fitting in the present work includes the initial condition, which is really important from both a conceptual and a practical point of view. On the other hand, our model predicts the  $a_{s1}$  and  $a_{s2}$  curves instead of using this data in the overall fitting.

Finally, some limitations can be pointed out in the operational method proposed to define the reversible and irreversible fractions, particularly in the early aliquots. After sampling, the aliquots were 25 min centrifuged and then processed by a sequential extraction (1 + 2 + 2 + 6 h with different reagents). Therefore it is possible that a fraction of the reversible sorbed tracer changed to the irreversible (or slowly reversible) bounded fraction. This could explain the observed discrepancies between the model predictions and the data, in the case of data points which corresponds to less than 1 h of contact time (Figs. 5 and 6).

An important conceptual limitation in the set of parameters proposed by the authors, for Co, is that  $k_{21} = 0$  (see Table 4). This directly implies that  $a_w/a_w(0) = e^{-k_{11}t}$ , i.e. the liquid phase concentration follows an exponential. But in the corresponding graph and data, the adsorption of radio-cobalt clearly shows two time scales, a fast initial uptake (which originally was not described) and a second more moderate. Therefore, the only possible interpretation for those coefficients is to describe the transfer from water as a simple exponential decay and then to explain the redistribution of the radionuclide inside the particles on the basis of indirect or operationally defined measurements. Another consequence for using  $k_{21} = 0$  (the only reversible channel to  $a_w$  in the *CRR* model) is that the model cannot describe any desorption from the particles to the water, which is refuted by their experimental results for the sequential extraction. Thus, particles released cobalt when clean water was mixed with the polluted particles. In that sense, Fig. 7

Table 5  
Desorbed  $^{60}\text{Co}^a$  by marine clean water after uptakes with different contact times

Time [days]	Released $^{60}\text{Co}$ fraction in water
0.01	0.051
0.03	0.051
0.11	0.043
1	0.024
2	0.009
6	0.000

<sup>a</sup> Experimental data from Børretzen and Salbu (2000).

Table 6  
Exponential and model's coefficients for  $^{109}\text{Cd}^a$

	Present work, $R^2 = 0.9988^d$				Børretzen and Salbu			
Uptake curve <sup>b</sup>	$t_1$	$t_2$	$A_1$	$A_2$				
	0.0064	1.839	0.222	0.723				
Box models <sup>c</sup>	$k_{11}$	$k_{21}$	$k_{12}$	$k_{22}$	$k_{11}$	$k_{21}$	$k_{12}$	$k_{22}$
<i>PRR</i>	34.427	121.68	0.649	0.038	0.23	0.064	0.28	0.006
<i>CRR</i>	35.076	119.43	2.249	0.039				

<sup>a</sup> Experiment from Børretzen and Salbu (2000).

<sup>b</sup> Parameters given in Eq. (2). The  $A_i$ 's are dimensionless,  $t_i$  are given in hours (obtained by fitting).

<sup>c</sup> Models and coefficients defined in Fig. 1.  $k_{ij}$  values in  $\text{days}^{-1}$ .

<sup>d</sup>  $R^2$  corresponds to the exponential fitting (Eq. (2)).

shows the prediction of our models (*CRR* and *PRR* models give the same result for  $a_w$ ). They can be compared with the author's reported values of cobalt released for each aliquot (in Table 5). In all the cases the corresponding values are in the same range although always higher in the model predictions. We note that possible artefacts in the experimental method (those processes occurring in samples between sorption and desorption experiments) are expected to increase the irreversibly bound fraction, and thus reducing desorption.

In the experiment performed with Cd, Børretzen and Salbu (2000) proposed the *PRR* model to explain the uptake trend. They defined  $a_{s2}$  as the amount of radionuclides released in the last step of the sequential extraction ( $\text{HNO}_3$  desorbed fraction), and all the previous steps were considered as  $a_{s1}$ . But if we use the  $a_w$  curve to predict the particle-associated compartments, the result leads to a better agreement when changing the definition of the operational fractions. Thus, we re-defined  $a_{s2}$  as the amount of tracer extracted by the two last steps ( $\text{NH}_4\text{Ac}$  pH 5 and  $\text{HNO}_3$ ), being  $a_{s1}$  the complementary fraction (Fig. 6a and Table 6). Then on the basis of the present work, it cannot be concluded that *PRR* model was better for cobalt or cadmium than the *CRR* one.

The experimental method proposed by those authors clearly marks a guideline for studying the uptake kinetics and reversibility. Nevertheless, the definition of the particle-associated compartments cannot be arbitrary, since they are not independent from the time course of concentrations in the dissolved phase.

## 5. Conclusions

The uptake of radionuclides by particulate matter is featured by a complex sorption that actually occurs in different steps. These processes can be described in terms of their characteristics times by a multi-exponential function representing the concentrations in water or in the particle-associated compartments. Such description can also be expressed by means of a multi-compartmental model, where the boxes represent the amount of radionuclides in the water and in the different sites on the particles. *PRR* and *CRR* models can be constructed providing the same analytical solution for the uptake curve (time course of tracer concentrations in the dissolved phase) and mathematically different (although often close) solutions for the solid-compartments.

Without questioning the practical use of these models, an important question arises about the physical meaning of the involved kinetic coefficients. Despite the experimental limitations in measuring solid-compartments, their operational definition can neither be arbitrary nor independent of the predictions based in the uptake curve itself.

The development of suitable uptake kinetic models requires a good time resolution in the experiment. Once the model parameters are found from the uptake curve, then the predictive value of the model should be checked against additional experiments. To avoid any artefact in the handling of samples between experiments, one on-line design is advisable. The design of specific experiments to unambiguously distinguish between *PRR* and *CRR* models is still an open question.

## References

Abril, J.M., 1998. Basic microscopic theory of the distribution, transfer and update kinetics of dissolved radionuclides by suspended particulate matter. Part I: theory development. *J. Environ. Radioact.* 41, 307–324.

- Benes, P., Cernik, M., 1992. Kinetics of radionuclide interaction with suspended solids in modelling the migration of radionuclides in rivers II. Effect of concentration of the solids and temperature. *J. Radioanal. Nucl. Chem.* 159, 187–200.
- Benes, P., Cernik, M., Slávik, O., 1994. Modelling the migration of  $^{137}\text{Cs}$  accidentally released into a small river. *J. Environ. Radioact.* 22, 279–293.
- Børretzen, P., Salbu, B., 2000. Estimation of apparent rate coefficients for radionuclides interacting with marine sediments from Novaya Zemlya. *Sci. Total Environ.* 262, 91–102.
- Børretzen, P., Salbu, B., 2002. Fixation of Cs to marine sediments estimated by a stochastic modelling approach. *J. Environ. Radioact.* 61, 1–20.
- Bunker, D.J., Smith, J.T., Lievens, F.R., Hilton, J., 2001. Kinetics of metal ion sorption on lake sediments – approaches to the analysis of experimental data. *Appl. Geochem.* 16, 651–658.
- Ciffroy, P., Garnier, J.M., Phan, M.K., 2001. Kinetics of the adsorption and desorption of radionuclides of Co, Mn, Cs, Fe, Ag and Cd in freshwater systems: experimental and modelling approaches. *J. Environ. Radioact.* 55, 71–91.
- Comans, R.N.J., Hockley, D.E., 1992. Kinetics of cesium sorption on illite. *Geochim. Cosmochim. Acta* 56, 1157–1164.
- El Mrabet, R., Abril, J.M., Manjón, G., García Tenorio, R., 2001. Experimental and modelling study of the Plutonium uptake by suspended matter in aquatic environments from southern Spain. *Water Res.* 35, 4184–4190.
- ENRESA, 2002. Estudios sobre los mecanismos de transferencia de radionucleidos entre los diversos compartimentos de la biosfera. Annual technical report produced by the University of Seville (contract OG-05/02) for ENRESA (I+D code: 774511 – 0770105) (in Spanish).
- Konoplev, A.V., Bulgakov, A.A., Popov, V.E., Bobovnikova, Ts.I., 1992. Behaviour of long-lived Chernobyl radionuclides in a soil–water system. *Analyst* 117, 1041–1047.
- Laïssaoui, A., Abril, J.M., Periañez, R., García-León, M., García Montañó, E., 1998. Kinetic transfer coefficients for radionuclides in estuarine waters: reference values from  $^{133}\text{Ba}$  and effects of salinity and suspended load concentration. *J. Radioanal. Nucl. Chem.* 237 (1–2), 55–61.
- Monte, L., Periañez, R., Kivva, S., Laptev, G., Angeli, G., Barros, H., Zheleznyak, M., 2006. Assessment of state-of-the-art models for predicting the remobilisation of radionuclides following the flooding of heavily contaminated areas: the case of Pripjat River floodplain. *J. Environ. Radioact.* 88, 267–288.
- Nyffler, U.P., Li, Y.H., Santschi, P.H., 1984. A kinetic approach to describe trace- element distribution between particles and solution in natural aquatic systems. *Geochim. Cosmochim. Acta* 48, 1513–1522.
- Periañez, R., Martínez-Aguirre, A., 1997. Uranium and thorium concentrations in an estuary affected by phosphate fertilizer processing: experimental results and a modelling study. *J. Environ. Radioact.* 35, 281–304.
- Periañez, R., Elliot, A.J., 2002. A particle-tracking method for simulating the dispersion of non-conservative radionuclides in coastal waters. *J. Environ. Radioact.* 58, 13–33.
- Sasina, N.V., Smith, J.T., Kudelsky, A.V., Wright, S.M., 2007. “Blind” testing of models for predicting the  $^{90}\text{Sr}$  activity concentration in river systems using post- Chernobyl monitoring data. *J. Environ. Radioact.* 92, 63–71.
- Smith, J.T., Comans, R.N.J., 1996. Modelling the diffusive transport and remobilisation of  $^{137}\text{Cs}$  in sediments: the effects of sorption kinetics and reversibility. *Geochim. Cosmochim. Acta* 60, 995–1004.
- Stephens, J.A., Ward Whicker, F., Ibrahim, S.A., 1998. Sorption of Cs and Sr to profundal sediments of Savannah River site reservoir. *J. Environ. Radioact.* 38, 293–331.